Neuropsychopharmacology (2013) 38, 1176–1188

www.neuropsychopharmacology.org

Ethanol Reduces Neuronal Excitability of Lateral Orbitofrontal Cortex Neurons Via a Glycine Receptor Dependent Mechanism

Kimberly A Badanich[1,2], Patrick J Mulholland[1,2], Jacob T Beckley[1,2], Heather Trantham-Davidson[1,2] and John J Woodward*[,1,2]

[1]Department of Neurosciences, Medical University of South Carolina, Charleston, SC, USA; [2]Department of Psychiatry and Behavioral Sciences, Center for Drug and Alcohol Programs, Medical University of South Carolina, Charleston, SC, USA

Trauma-induced damage to the orbitofrontal cortex (OFC) often results in behavioral inflexibility and impaired judgment. Human alcoholics exhibit similar cognitive deficits suggesting that OFC neurons are susceptible to alcohol-induced dysfunction. A previous study from this laboratory examined OFC mediated cognitive behaviors in mice and showed that behavioral flexibility during a reversal learning discrimination task was reduced in alcohol-dependent mice. Despite these intriguing findings, the actions of alcohol on OFC neuron function are unknown. To address this issue, slices containing the lateral OFC (lOFC) were prepared from adult C57BL/6J mice and whole-cell patch clamp electrophysiology was used to characterize the effects of ethanol (EtOH) on neuronal function. EtOH (66 mM) had no effect on AMPA-mediated EPSCs but decreased those mediated by NMDA receptors. EtOH (11–66 mM) also decreased current-evoked spike firing and this was accompanied by a decrease in input resistance and a modest hyperpolarization. EtOH inhibition of spike firing was prevented by the $GABA_A$ antagonist picrotoxin, but EtOH had no effect on evoked or spontaneous GABA IPSCs. EtOH increased the holding current of voltage-clamped neurons and this action was blocked by picrotoxin but not the more selective $GABA_A$ antagonist biccuculine. The glycine receptor antagonist strychnine also prevented EtOH's effect on holding current and spike firing, and western blotting revealed the presence of glycine receptors in lOFC. Overall, these results suggest that acutely, EtOH may reduce lOFC function via a glycine receptor dependent process and this may trigger neuroadaptive mechanisms that contribute to the impairment of OFC-dependent behaviors in alcohol-dependent subjects.
Neuropsychopharmacology (2013) **38,** 1176–1188; doi:10.1038/npp.2013.12; published online 6 February 2013

Keywords: alcohol; patch-clamp electrophysiology; glycine; tonic current; NMDA; $GABA_A$

INTRODUCTION

The orbitofrontal cortex (OFC), a region within the prefrontal cortex (PFC), mediates several aspects of learning, including choice behavior (Boettiger *et al*, 2007; Bokura *et al*, 2001; Ramus and Eichenbaum, 2000; Roesch *et al*, 2007a; Schoenbaum *et al*, 1998), reversal learning (Dalley *et al*, 2004; McGaughy *et al*, 2008; Roesch *et al*, 2007b; Thorpe *et al*, 1983) and the development of expectancies/predictions (Ito *et al*, 2001; Tremblay and Schultz, 1999) about appetitive and aversive stimuli. Current thinking suggests that the OFC, with its extensive array of sensory and limbic derived inputs, mediates learning processes and specifically choice behavior by providing a place for incoming information to be integrated and by attributing salience to relevant environmental cues. Dysfunction of the OFC is associated with behavioral inflexibility and an inability to anticipate consequences often leading to poor judgment in humans (Bechara *et al*, 1998) and in OFC lesioned rodents (Dalley *et al*, 2004; McGaughy *et al*, 2008). Specifically, damage to the orbitofrontal-subcortical circuit disrupts behavioral inhibition (Cummings, 1995) and lesions to lateral and ventral OFC, but not the mPFC, disrupt reversal learning (Bissonette *et al*, 2008). Human alcoholics often display symptoms similar to patients with OFC damage, including deficits in behavioral inhibition (Verdejo-Garcia *et al*, 2006) and measures of impulsivity/perseveration (Hill *et al*, 2009; Tanabe *et al*, 2009). Chronic alcohol exposure has also been shown to disrupt behavioral flexibility in experimental models of alcohol dependence. In a previous study from this lab, (Badanich *et al*, 2011), alcohol-dependent mice showed impaired performance on a reversal learning task that requires an intact OFC (Bissonette *et al*, 2008). Together with reports from human alcoholics, these findings suggest that OFC neurons may be particularly sensitive to alcohol.

To date, most studies of OFC function have used *in vivo* recordings to monitor responses in alcohol naive behaving

*Correspondence: Dr JJ Woodward, Department of Neurosciences, Medical University of South Carolina, 67 President Street, IOP471, Charleston, SC 29425, USA, Tel: +843 792 5225, Fax: +843 792 7353, E-mail: woodward@musc.edu
Received 28 November 2012; revised 5 January 2013; accepted 7 January 2013; accepted article preview online 11 January 2013

monkeys/rodents. OFC neurons encode physical properties of visual and textual cues as well as motivational valence (Tremblay and Schultz, 1999) and predictive nature of reward contingencies (Ikeda *et al*, 1996; Ramus and Eichenbaum, 2000; Schoenbaum *et al*, 1998; Schoenbaum and Eichenbaum, 1995; Schultz *et al*, 2000) during decision-making tasks. Furthermore, primates and rodents show selective increases in firing of OFC neurons in response to a go response and these same neurons return to a baseline rate of firing following reversal learning (Roesch *et al*, 2007b; Thorpe *et al*, 1983). These data indicate that neuronal activity in the OFC mediates higher order cognitive function specifically related to reversal learning and tasks that require behavioral flexibility.

Despite evidence from both human and animal studies implicating the OFC as an important target for ethanol (EtOH), there is little known regarding the actions of EtOH on OFC neuron activity at the cellular level. In the present study, we characterize the effects of acute EtOH on neurons in the lateral OFC (lOFC) from adult mice to better understand the impact of EtOH exposure on behavioral flexibility and other OFC-dependent behaviors. EtOH concentrations from 11–66 mM were used to model relevant blood alcohol concentrations ($\sim$0.05–0.31%) that are a result from drinking. Results from these experiments show that OFC neuron firing is reduced by relatively low concentrations of EtOH via a glycine-receptor-dependent mechanism while higher concentrations reduce NMDA evoked synaptic currents.

MATERIALS AND METHODS

Experimental Subjects

C57BL/6J male mice purchased from Jackson Laboratories (Bar Harbor, ME) at 7 weeks of age were used in the electrophysiology experiments. After arrival, mice were group-housed (4/cage) and allowed to acclimate to the colony room for at least 1 week. Mice were housed in a temperature and humidity controlled AAALAC-approved facility, with ad libitum access to food and water. The animal housing room was maintained under a 12 h light/dark cycle (lights on at 600 h). At the start of the electrophysiology experiments, mice ranged from 8–12 weeks old and weighed an average of 25 g (range: 20–30 g). The care and use of mice was conducted under guidelines for animal care approved by the Medical University of South Carolina's Institutional Animal Care and Use Committee and the NIH Guide for the Care and Use of Laboratory Animals (NIH Publication No.: 80–23, revised 1996).

Preparation of Brain Slices

The lateral portion of the OFC was selected for recordings as previous reports suggested that lesions of the lateral/ventral OFC disrupt reversal learning (Bissonette *et al*, 2008) and that the lOFC, but not the mOFC, is associated with the suppression of a previously rewarded response (Adinoff, 2004). Furthermore, changes in dendritic morphology have been observed specifically in the lOFC following exposure to stress and psychostimulants suggesting that these neurons may be especially sensitive to drug exposure (Dias-Ferreira *et al*, 2009; Liston *et al*, 2006). Acute brain slices containing the lOFC were prepared for whole-cell patch-clamp electrophysiology experiments. Mice were deeply anesthetized with sodium pentobarbital and transcardially perfused through the ascending aorta with ice-cold (4 °C) oxygenated (95% O_2, 5% CO_2) sucrose containing buffer (in mM; 200 sucrose, 1.9 KCl, 1.2 NaH_2PO_4, 6 $MgCl_2$, 0.5 $CaCl_2$, 0.4 ascorbate, 10 glucose, 25 $NaHCO_3$, adjusted to 305–315 mOsm). Following perfusion, mouse brains were immediately removed, blocked for the frontal cortex and sectioned using a Leica VT1000S vibratome (Buffalo Grove, IL) maintained at 4 °C. Coronal slices (300 μm) containing the lOFC were immediately placed in a holding chamber and incubated at 34 °C for 30 min in oxygenated artificial cerebral spinal fluid (aCSF, in mM; 125 NaCl, 2.5 KCl, 1.25 NaH_2PO_4, 1.3 $MgCl_2$, 2.0 $CaCl_2$, 0.4 ascorbate, 10 glucose, 25 $NaHCO_3$, adjusted to 305–315 mOsm). Slices were then kept at room temperature for at least 30 min before recording.

Whole-Cell Patch-Clamp Electrophysiology

Slices were placed in a temperature controlled recording chamber (34 °C) and perfused with oxygenated aCSF at a flow rate of 2 ml/min. Recordings were localized to deep layers of the lOFC (Figure 1a) previously reported to produce deficits in reversal learning following lesioning (Bissonette *et al*, 2008; Franklin and Paxinos, 2008). Most recordings were from neurons that were approximately 500–750 μm from the rhinal fissure. Neurons from the lOFC were identified using an Olympus BX51W1 microscope (Center Valley, PA) equipped with infrared Dodt gradient contrast imaging (Luigs and Neumann, Ratingen, Germany). Thin-wall borosilicate glass electrodes (OD = 1.5 mm, ID = 1.17 mm) were pulled on a Sutter Instrument Micropipette Puller (Novato, CA) and had tip resistances ranging from 1.2–7.7 mΩ. Patch pipettes were filled with an internal solution (see below for recipes) and slowly lowered onto the cell body of a neuron to obtain a seal ($>$1 GΩ) followed by breakthrough to gain whole-cell access. Whole-cell patch-clamp electrophysiological recordings were carried out using an Axon MultiClamp 700B amplifier (Molecular Devices, Union City, CA). For all recordings, events were filtered at 4 kHz and digitized at a sampling rate of 10 kHz. Approximately 5–10 min were allowed for each neuron to stabilize before recordings commenced. Electrophysiological recordings were divided into three recording epochs, including a 5–10 min baseline, 10 min treatment, and 10 min washout session. Each EtOH treatment session was compared with its own baseline and served as a within-subjects control. Except for the tonic current experiments, EtOH (11–66 mM) was added to the aCSF perfusion solution and bath applied for all treatment sessions. Healthy cells and reliable recordings were identified by monitoring series resistances (Rs) over the course of the recording session. Recordings with Rs greater than 30 MΩ or that fluctuated by more than 25% over the course of the experiment were eliminated from final analyses.

Synaptic GABA and NMDA currents. A cesium chloride internal pipette solution (in mM; 120 CsCl, 10 HEPES, 2 $MgCl_2$, 1 EGTA, 2 NaATP, 0.3 NaGTP, 1 QX-314, 0.2%

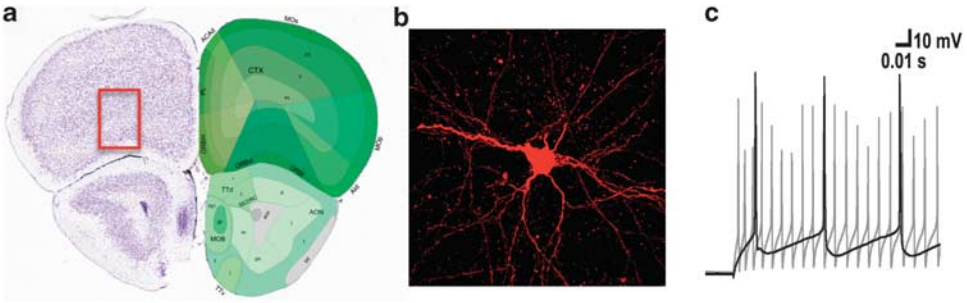

d

	Resting membrane potential (mV)	Input resistance (MΩ)	Action potential threshold (mV)	Action potential height (mV)	Action potential width (ms)	Action potential rise (ms)	Afterhyper-polarization (pA)
RS	-67.5 ± 0.5	80.4 ± 4.1	-38.2 ± 0.9	73.4 ± 3.6	0.95 ± 0.06	0.41 ± 0.03	10.3 ± 0.8
FS	-70.1 ± 4.3	162.4 ± 37.2	-46.7 ± 0.5	61.6 ± 7.4	0.36 ± 0.05	0.35 ± 0.06	17.0 ± 5.6

Figure 1 Neurophysiological characteristics of lOFC neurons. (a) Coronal slice from adult mouse brain atlas (Allen Mouse Brain Atlas (Internet). Seattle (WA): Allen Institute for Brain Science. 2009. Available from: http://mouse.brain-map.org). The boundaries of the targeted recording site (lateral OFC) are outlined in the red box. (b) Confocal image of biocytin filled regular spiking lOFC neuron. (c) Example traces of regular spiking (RS) and fast spiking (FS) neurons during current injection. Gray trace = fast spiking; Black trace = regular spiking. (d) Electrophysiological characteristics of OFC neurons recorded under control conditions. For each dependent measure, raw scores are presented as mean ± SEM. $N = 25$ (RS), 4(FS).

biocytin, pH = 7.4, adjusted to 294 mOsm) was used to record synaptic glutamate and GABA mediated events. A concentric bipolar stimulating microelectrode (World Precision Instruments, Sarasota, FL) was placed in the lOFC adjacent to and in close proximity to the recording site. Stimulus pulses were delivered at a rate of 0.01 Hz and ranged from 10–1,025 μAn in intensity to elicit a stable and submaximal evoked current. For evoked AMPA and NMDA EPSCs, the $GABA_A$ antagonist, picrotoxin (100 μM), and DL-AP5 (100 μM) or NBQX (10 μM), respectively were added to the aCSF perfusion solution. AMPA EPSCs were measured at a holding potential of −70 mV while NMDA EPSCs were acquired while holding the neuron at +40 mV to relieve the magnesium block on the receptor. For evoked GABA IPSCs, the NMDA receptor antagonist, DL-AP5 (100 μM), and the AMPA receptor antagonist, NBQX (10 μM), were added to the aCSF perfusion solution and the neuron was voltage clamped at −70 mV. Amplitude (pA) and area (pA/ms) of synaptic currents were measured to determine the effects of EtOH (11–66 mM) on evoked GABA IPSCs and evoked AMPA and NMDA EPSCs. In a separate set of experiments, spontaneous GABA-mediated IPSCs were measured in the same manner as evoked GABA currents, except that no stimulating pulse was applied to the slice. GABA IPSCs were identified using a sliding template algorithm in AxographX software (Axograph Scientific, New South Wales, Australia). The amplitude (pA) and frequency (ms) of spontaneous GABA IPSCs were measured by comparing cumulative probability curves and overall means for each recording session (baseline, treatment, washout).

Intrinsic excitability experiments. For determining the effects of EtOH on spike firing, current-clamp recordings were performed using a potassium gluconate internal pipette solution (in mM, 120 KGluc, 10 KCl, 10 HEPES, 2 $MgCl_2$, 1 EGTA, 2 NaATP, 0.3 NaGTP, 0.2% biocytin, adjusted to 294 mOsm, pH = 7.4). Current injections (100–300 pA) were used to evoke action potential firing in lOFC neurons and neuron excitability was evaluated before, during and after EtOH exposure. A brief depolarizing current that did not elicit action potentials (50 pA) was injected before each epoch to monitor input resistance. To examine the effects of EtOH on GABA and glycine receptor function, the $GABA_A$/glycine antagonist picrotoxin (100 μM) or the glycine antagonist strychnine (1 μM) was added to the aCSF perfusion solution and bath applied throughout the entire recording session (baseline, treatment, washout). Recordings were analyzed for resting membrane potential (mV), input resistance (MΩ), and action potential (AP) threshold (mV), height (mV), half width (ms), rise time (ms), and frequency (no. spikes). Resting membrane potentials were not adjusted for the liquid junction potential error (~12.2 mV).

Tonic currents. Changes in tonic current during exposure to EtOH or receptor blockers were measured by recording the holding current of a neuron voltage clamped at −60 mV. A cesium chloride internal pipette solution (in mM; 120 CsCl, 10 HEPES, 2 $MgCl_2$, 1 EGTA, 2 NaATP, 0.3 NaGTP, 1 QX-314, 0.2% biocytin, pH = 7.4, adjusted to 294 mOsm) was specifically used to amplify inward currents while measuring changes in holding current. In order to match the recording conditions used during spiking experiments, no pharmacological blocking agents were added to the recording aCSF in the tonic current experiments. Baseline recordings were conducted until the holding current was stable (2–3 min). In these experiments, EtOH and various pharmacological agents were locally applied to the patched neuron using a gravity-fed perfusion barrel positioned just above the recording site. Specifically, separate glass syringes were used as perfusion reservoirs and a stopcock controlled the flow of each drug solution

into a four-way manifold connected to a square quartz perfusion tube (0.6 mm ID; Warner Instruments, Hamden, CT). To control for this method of drug application, aCSF was locally applied during the baseline and washout recording sessions in control experiments. EtOH (66 mM) was locally applied for 4 min in all experiments. A series of additional experiments were conducted to determine EtOH's mode of action on tonic current. In these experiments, specific pharmacological agents were co-applied locally with EtOH to the brain slice using the system described above. These included the $GABA_A$ receptor antagonist bicuculline (50 μM), the $GABA_A$/glycine receptor antagonist picrotoxin (100 μM), or the glycine receptor antagonist strychnine (1 μM). The effects of exogenous glycine (300 μM) and strychnine (1 μM) on tonic current were also measured. For analysis of tonic current, baseline holding currents were set to zero and changes in current during pharmacological treatments were measured as change from baseline. Holding current in each condition was determined by averaging 10 different epochs in a 10 s area of the trace where no spontaneous synaptic currents were observed. Changes in current produced by test compounds were always compared with the preceding treatment session within the same neuron.

Histology and Confocal Microscopy

Slices containing the lOFC were fixed for 48 h in 4% PFA, rinsed in 0.01 M phosphate buffered saline (PBS), and then were incubated in 5% normal goat serum with 0.1% Triton-X for 7 min. Slices were incubated in Avidin TexasRed for 24 h at 4 °C., washed in PBS, and mounted on glass slides. Slides were coverslipped using Prolong Antifade (Life Technologies; Grand Island, NY) and imaged using a Zeiss LSM 510 confocal microscope (Thornwood, NY) with a 63X oil objective.

Western Blotting

The expression of glycine receptor subunits was analyzed by western blotting. Briefly, animals were rapidly euthanized by decapitation, and brains and spinal cord were immediately immersed for 1–2 min in ice-cold PBS (pH 7.4). Brains were sectioned into 1 mm thick coronal slices using an adult mouse brain matrix (ASI Instruments, Warren, MI) and punches were taken from the lOFC, hippocampus, reticular formation, and spinal cord and briefly sonicated in 2% LDS. An aliquot of each homogenate was diluted with NuPAGE 4 × LDS sample loading buffer (Invitrogen, Carlsbad, CA; pH 8.5) containing 500 mM dithiothreitol, and samples were denatured for 10 min at 70 °C. Twenty microgram of each sample was separated using the Bis-Tris (375 mM resolving buffer and 125 mM stacking buffer, pH 6.4; 7.5% acrylamide) discontinuous buffer system with MOPS electrophoresis buffer (50 mM MOPS, 50 mM Tris, 0.1% SDS, 1 mM EDTA, pH 7.7). Protein was then transferred to Immobilon-P PVDF membranes (Millipore, Bedford, MA) using a semi-dry transfer apparatus. After transfer, blots were washed with PBS containing 0.1% Tween 20 (PBST) and then blocked with PBST containing 5% nonfat dried milk (NFDM) for 1 h at room temperature with agitation. The membranes were then incubated overnight at 4 °C with a primary antibody directed against glycine receptor alpha subunits (clone mAb4a, Synaptic Systems, Goettingen, Germany) diluted in PBST containing 0.5% NFDM and washed in PBST before 1 h incubation at room temperature with horseradish peroxidase conjugated secondary antibodies diluted 1 : 2000 in PBST. Membranes received a final wash in PBST and the antigen-antibody complex was detected by enhanced chemiluminescence using a ChemiDoc MP Imaging system (Bio-Rad Laboratories, Hercules, CA). The band corresponding to the appropriate size subunit was quantified by mean optical density using computer-assisted densitometry with ImageJ v1.41 (National Institutes of Health, USA).

Statistical Analysis

Separate analyses of variance (ANOVA) were used to analyze each experiment. To analyze the effects of EtOH on OFC neuron action potential characteristics, a 5×3 mixed factor ANOVA with Treatment (control, 11 mM EtOH, 33 mM EtOH, 66 mM EtOH, 33 mM EtOH + 100 μM picro) as the between subjects factor and Session (baseline, treatment, washout) as the repeated measure was used. Dependent variables were resting membrane potential (mV), input resistance (MΩ), and action potential (AP) threshold (mV), height (mV), half width (ms), rise time (ms) and frequency (no. spikes). For GABA IPSCs (evoked and spontaneous) and evoked AMPA and NMDA EPSCs, data were analyzed using a 3×3 mixed factor ANOVA with Treatment (11, 33, 66 mM EtOH) as the between subjects factor and Session (baseline, treatment, washout) as the repeated measure. Amplitude (pA) and area (pA/ms) were measured for evoked GABA IPSCs and AMPA and NMDA EPSCs while amplitude (pA) and inter-event interval (IEI, ms) were measured for spontaneous GABA IPSCs. Additionally, cumulative probability curves were plotted to determine if there were effects of Treatment on spontaneous GABA IPSCs amplitude or inter-event interval. A one-way ANOVA with Treatment as the between subjects factor was used to analyze changes in holding current (pA). Nine treatment groups were compared in this analysis. Finally, the effects of the NR2B receptor subunit Ro-25-6931 on evoked NMDA EPSCs were analyzed by a one-way ANOVA with Treatment (baseline, Ro-25-6931, RO 25-6931 + EtOH) as the repeated measure. For all analyses, post-hoc analyses were performed by isolating simple effects and by using Fisher's least significant difference (LSD) test (significance level set at $P < 0.05$).

RESULTS

Figure 1 summarizes the location of the recording site in the lateral orbitofrontal cortex (lOFC) and the properties of the two types of neurons that were identified during whole-cell recordings. The majority of neurons were large cells (Figure 1b) with input resistance < 100 MΩ and a regular pattern of spiking upon current injection (Figures 1c and d). A small subset of neurons was characterized by higher input resistance, greater frequency of current-evoked spiking (> 70 spikes/500 ms), and a deep after-hyperpolarization following each action potential (Figures 1c and d). Given

that only a few recordings from fast-spiking neurons were obtained, all further analyses were performed on large regular-spiking lOFC neurons.

Effects of EtOH on AMPA and NMDA EPSCs

EtOH inhibits NMDA currents in a variety of brain regions, including the amygdala (Roberto *et al*, 2004) and PFC (Weitlauf and Woodward, 2008) while those mediated by AMPA receptors are generally less affected. In lOFC neurons, 66 mM EtOH ($\sim$0.3% blood EtOH concentration; BEC) significantly (Treatment $\times$ Session interaction $F(4, 48) = 2.89$, $P < 0.05$) inhibited currents mediated by NMDA receptors (Figures 2a and b). This effect fully reversed upon washout and no rebound in current amplitude was observed. Lower concentrations of EtOH (11 mM, 33 mM) had no significant effects on stimulus-evoked NMDA EPSCs in lOFC neurons (Figure 2a and b). In some brain regions such as the bed nucleus of the stria terminalis (BNST), EtOH inhibition of NMDA EPSCs appears to require the GluN2B subunit as blocking these receptors occludes any further action by EtOH (Kash *et al*, 2008). To determine whether lOFC neurons are similar to those in BNST, NMDA EPSCs were recorded in the absence and presence of the selective GluN2B subunit antagonist Ro-25-6981. By itself, Ro-25-6981 (2.5 μM) significantly reduced the amplitude of stimulus evoked NMDA EPSCs by $\sim$25%. (Figures 2c and d; $F(2, 29) = 36.60$, $P < 0.05$). In the presence of Ro-25-6981,

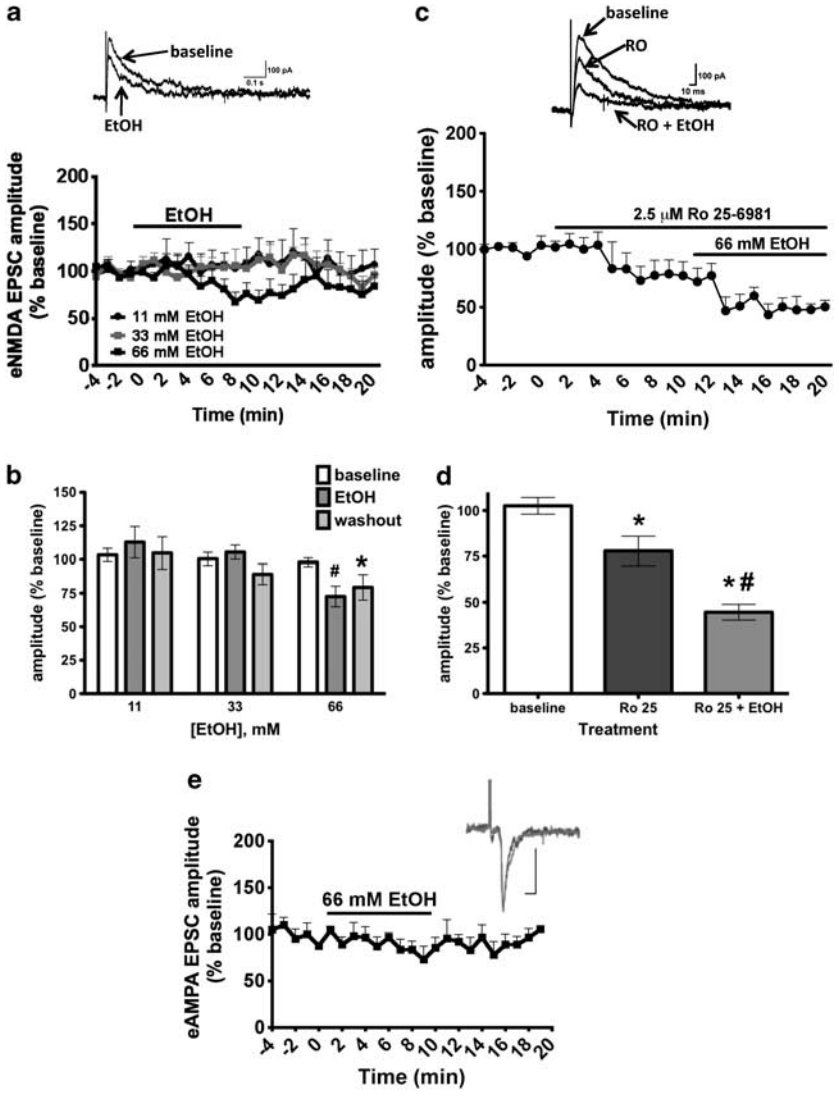

Figure 2 Acute EtOH inhibits stimulus-evoked NMDA but not AMPA EPSCs in lOFC neurons. (a) Time-course effects of EtOH on amplitude of evoked NMDA and AMPA EPSCs. Data shown are percent of pre-EtOH baseline. Representative traces show NMDA currents recorded at +40 mV in the absence and presence of 66 mM EtOH. (b) Summary chart shows amplitude of NMDA EPSCs during the last 2 min of each recording epoch (baseline, treatment, washout) for 11, 33, and 66 mM EtOH. Only the highest EtOH concentration (66 mM) inhibited NMDA EPSC amplitude. Symbols: * = differs from baseline. # = differs from baseline, 11, 33 mM EtOH. (c) Time-course effects of the NR2B-NMDA receptor antagonist RO 25-6981 and EtOH on amplitudes of evoked NMDA EPSCs. Example trace shows effects of RO 25-6981 alone and in combination with EtOH on evoked NMDA EPSCs. (d) Summary chart shows amplitude (as percent of pre-drug control) for evoked NMDA EPSCs during the last 2 min of each recording epoch (baseline, RO 25-6981, RO 25-6981 + EtOH). Symbols: * = differs from baseline. # = differs from RO 25-6981. (e) EtOH (66 mM) has no effect on amplitude of evoked AMPA EPSCs. Data shown are percent of pre-EtOH baseline. Representative traces show AMPA currents in the absence (blue) and presence (red) of 66 mM EtOH. All bars and data points represent mean ± SEM. $N = 4$–7 for each treatment group. A color reproduction of this figure is available on the *Neuropsychopharmacology* journal online.

EtOH (66 mM) produced a further reduction in the amplitude of NMDA EPSCs ($P<0.05$) and this inhibition was similar in the absence or presence of the GluN2B blocker (Figures 2b and d). These data suggest that although lOFC neurons express significant amounts of GluN2B containing receptors, other EtOH-sensitive NMDA receptors are also present. In contrast to its effects on NMDA currents, EtOH (66 mM) had little effect on AMPA-mediated EPSCs (Figure 2e).

Effects of EtOH on $GABA_A$ Responses

In addition to inhibiting NMDA-mediated responses, EtOH has been shown to augment signaling by $GABA_A$ receptors in certain brain regions (Weiner and Valenzuela, 2006). To determine if EtOH modulates synaptic $GABA_A$ receptors on lOFC neurons, cells were recorded in voltage-clamp mode with a high-chloride containing internal solution and stimulus-evoked GABA IPSCs were generated. As shown in Figure 3, there were no significant effects of EtOH (11–66 mM) on the area of evoked GABA IPSCs ($F(4, 66)=0.47$, $P>0.05$) or on the peak of these currents (data not shown). In some brain areas, EtOH's effect on GABA mediated events is mediated by an increase in the presynaptic release of GABA rather than a direct effect on the receptor itself (see Weiner and Valenzuela, 2006). To examine this possibility more closely, we monitored spontaneous GABA IPSCs in the absence and presence of EtOH. Similar to that observed for evoked responses, there were no effects of EtOH (11–66 mM) on the amplitude (Figure 4; $F(4, 28)=0.11$, $P>0.05$) or frequency ($F(4,28)=1.19$, $P>0.05$) of spontaneous GABA IPSCs.

Effects of EtOH on OFC Neuron Excitability

To determine the effects of EtOH on the intrinsic excitability of OFC neurons, cells were recorded in current-clamp mode using a low chloride-containing internal solution and action potentials were monitored during brief periods of current injection. These recordings were done in the absence of receptor blockers except where indicated. EtOH (11–66 mM) had little effect on the properties of individual APs, including action potential threshold (Treatment × Session: $F(8, 90)=1.46$, $P>0.05$), half width (Treatment × Session: $F(8, 90)=0.85$, $P>0.05$), rise time (Treatment × Session: $F(8, 90)=1.96$, $P>0.05$), or the size of the after-hyperpolarization (Treatment × Session: $F(8, 90)=0.96$, $P>0.05$). Although there was a significant Treatment × Session interaction for action potential height (Treatment × Session: $F(8, 90)=6.89$, $P<0.05$), there were no significant differences between baseline and EtOH treatment conditions ($P>0.05$). There was also a trend towards EtOH causing a hyperpolarization of the resting membrane potential, however, this effect did not quite reach statistical significance in these studies (mV; Treatment × Session: $F(8, 90)=1.98$, $P=0.056$).

Despite its lack of effect on AP properties, EtOH significantly reduced the frequency of OFC neuron spiking (Treatment × Session: $F(8, 90)=3.35$, $P<0.05$). As shown in Figure 5, all three EtOH concentrations tested (11, 33, 66 mM) produced a time-dependent decrease in the frequency of current-evoked spiking in OFC neurons as compared with control baseline values (Figure 5b). Specifically, EtOH decreased firing frequency to 57, 49 and 49% of baseline for 11 mM, 33 mM and 66 mM EtOH, respectively (Figure 5c, $P<0.05$). Both 33 and 66 mM EtOH also significantly decreased spike firing relative to the between subjects control group (no EtOH group; $P<0.05$), Although the time of onset and rate of the EtOH-induced decrease in spike firing appeared to be concentration dependent, there were no statistical differences between the three EtOH exposure groups ($P>0.05$) at the end of the perfusion period. Once EtOH was removed from the perfusion bath, spike frequency returned to baseline levels during the washout recording session (Figures 5b and c).

EtOH inhibition of spike firing may result from enhanced GABAergic inhibition as reported for central amygdala (Roberto *et al*, 2003). However, as reported above, EtOH had no significant effect on $GABA_A$-mediated IPSC amplitude or frequency. GABA also activates extrasynaptic receptors following spillover of GABA from release sites (Glykys *et al*, 2007; Wei *et al*, 2004) or accumulation of GABA in the extracellular space. To test whether $GABA_A$

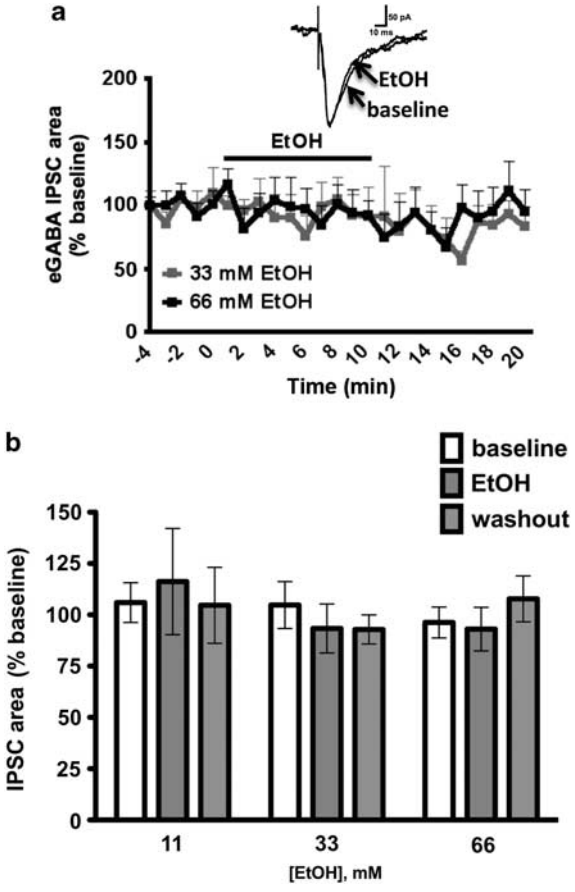

Figure 3 Acute EtOH does not alter evoked GABA IPSCs in lOFC neurons. (a) Time-course effects of EtOH on amplitude evoked GABA IPSCs (normalized to % of pre-EtOH baseline). Example trace shows no change in amplitude during exposure to 66 mM EtOH. (b) Summary chart showing amplitude of GABA IPSCs during the last 2 min of each epoch (baseline, treatment, washout) are shown for 11, 33, and 66 mM EtOH. There were no significant differences in amplitude for any of the Dose or Session groups. All bars and data points represent mean ± SEM. $N=5$–6 for each treatment group.

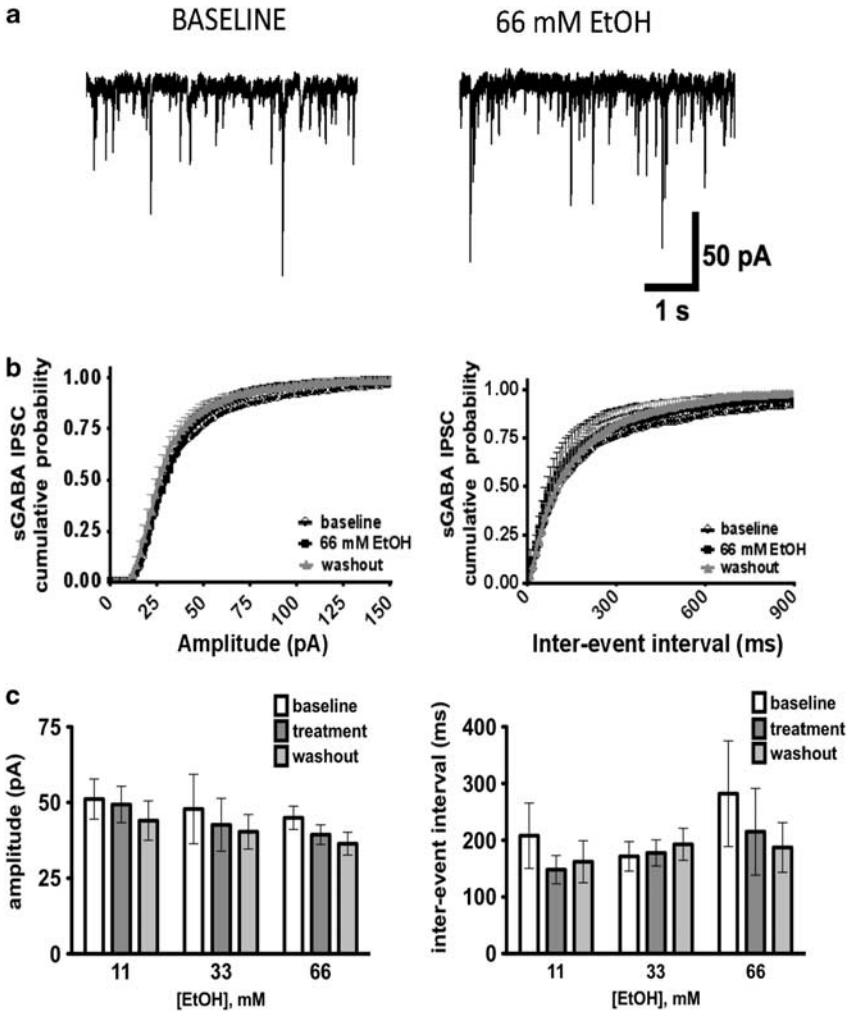

Figure 4 Acute EtOH does not alter spontaneous GABA IPSCs in lOFC neurons. (a) Representative traces showing spontaneous GABA IPSCs in the absence (left) and presence of 66 mM EtOH (right). (b) Cumulative probability curves for amplitude (left) and inter-event-interval (right) of spontaneous GABA IPSCs. Curves represent data collected during baseline, 66 mM EtOH and washout recording epochs. (c) Summary charts showing amplitude (left) and inter-event interval (right) for spontaneous GABA IPSCs during the last 2 min of each recording epoch (baseline, treatment, washout) are shown for 11, 33, and 66 mM EtOH. There were no significant differences in amplitude or inter-event interval for any of the Dose or Session groups. All bars and data points represent mean ± SEM. $N = 5$–7 for each treatment group.

signaling is involved in EtOH's effect on spike firing, recordings were performed in the presence of the $GABA_A$ receptor antagonist picrotoxin (100 μM). With picrotoxin present, EtOH (33 mM) no longer affected current-evoked spiking of lOFC neurons (Figures 5 a–c). These data suggest that EtOH may enhance a chloride-dependent $GABA_A$ receptor mediated current resulting in a decrease in the overall input resistance of the recorded neuron. All control groups had similar input resistance values ($P > 0.05$) before EtOH exposure and values were normalized to 100% in order to better show changes induced by EtOH. As predicted, the time-dependent decrease in spiking by EtOH (Figure 5b) was accompanied by decreases in input resistance (Figure 5d) as compared with the within-subjects control baseline values (Figure 5e (Treatment × Session: $F(8, 82) = 2.34$, $P < 0.05$)). As with spiking, all three EtOH concentrations tested (11, 33, 66 mM) produced a similar decrease in input resistance (78, 83 and 71% of baseline for 11, 33 and 66 mM EtOH, respectively) and these values were not statistically different between the three EtOH groups ($P > 0.05$). Both 11 and 66 mM EtOH also significantly decreased input resistances relative to the between subjects control group (no EtOH group; $P < 0.05$). Consistent with that observed for spike firing, picrotoxin blocked EtOH's effect on input resistance (Figures 5d and e; within subjects control, $P > 0.05$). During the 10 min washout period following EtOH exposure, input resistance values did not completely return to baseline levels for the 33 mM EtOH group (Figure 5e; $P < 0.05$) while values were slightly above baseline levels in the 11 mM EtOH group (Figure 5e; $P < 0.05$).

Effects of EtOH on Extrasynaptic GABA and Glycine Receptor Function

EtOH's lack of effect on evoked and spontaneous GABA IPSCs suggests that synaptic $GABA_A$ receptors do not have a role in EtOH's inhibition of spike firing. As mentioned above, in addition to synaptic receptors, GABA also activates extrasynaptic GABA receptors producing a tonic

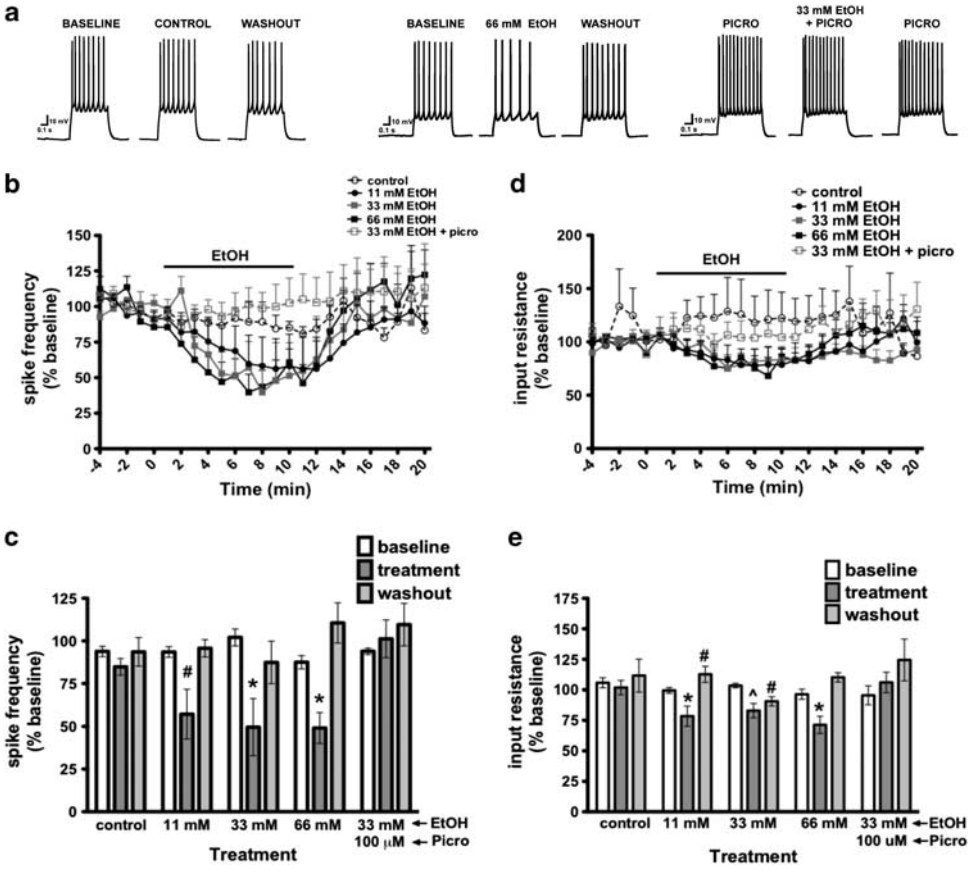

Figure 5 EtOH inhibits current-induced spiking in lOFC neurons. (a) Representative traces showing spiking under control conditions (left panel) and during application of EtOH (66 mM; middle panel) or EtOH (33 mM) and the GABA antagonist, picrotoxin (right panel). Time-course effects of EtOH on (b) spike frequency and (c) input resistance for the entire recording session for each of the treatment groups (control, 11, 33, 66 mM EtOH and 33 mM EtOH + 100 mM picrotoxin). Data are presented as percent of pre-EtOH baseline. Summary charts showing spike frequency (d) or input resistance (e) during the last 2 min of each recording epoch (baseline, treatment, washout) for each of the treatment groups. Picrotoxin blocked acute EtOH-mediated decrease in spike frequency and input resistance. Symbols: * = differs from all other groups. # = differs from control, baseline, washout; ^ = differs from picro baseline. All bars and data points represent mean ± SEM. $N = 5$ for each treatment group.

current that can influence neuronal excitability (Glykys *et al*, 2007; Wei *et al*, 2004). To directly examine the role of extrasynaptic $GABA_A$ receptors in EtOH action, we monitored holding current before and during local application of EtOH and $GABA_A$ receptor blockers. These experiments were done in the absence of any bath-applied pharmacological blocking agents in order to match the recording conditions used under the spiking experiments described above. Gaussian curves demonstrating ethanol-mediated increases (leftward shift) in holding current are depicted in Figures 6 a1–a3. Results from each experiment are summarized in Figures 6g and h and show a significant effect of Treatment Group ($F(8, 52) = 3.27$, $P < 0.05$). As shown in Figures 6a and h, EtOH (66 mM) induced a significant increase in the holding current of lOFC neurons and this change reversed during washout ($P < 0.05$). The EtOH-induced increase in holding current effect was prevented by picrotoxin that by itself reduced the holding current suggesting that lOFC neurons express a tonic GABA-mediated current (Figures 6b, g and h; $P < 0.05$). As the effects of picrotoxin on holding current were slow to recover, we repeated this experiment with bicucculine, a competitive and reversible inhibitor of $GABA_A$ receptors. Bicucculine alone also reduced the holding current (Figure 6c and g; $P < 0.05$), but did not consistently prevent the increase in holding current by EtOH (Figure 6h; $P > 0.05$). Although bicucculine is relatively selective for $GABA_A$ receptors, picrotoxin inhibits other ligand-gated ion channels, including those activated by glycine (Wang *et al*, 2006). Local application of the selective glycine receptor antagonist strychnine had no significant effect on the holding current (Figures 6d and g) but completely blocked that induced by EtOH (Figures 6d and h; $P < 0.05$). Together, these data suggest that lOFC neurons express both $GABA_A$ and glycine receptors, but only those currents gated by glycine are sensitive to EtOH. The lack of effect of strychnine alone on holding current may reflect a low expression of glycine receptors or the ability of glycine transporters to maintain extracellular levels of glycine at low levels. To examine whether the lOFC expresses glycine receptors, western blotting was performed on tissue punches using an antibody that recognizes all four alpha subunits of the glycine receptor. Compared with spinal cord and brain stem tissue, lOFC showed a modest but significant amount of immunoreactivity for glycine receptor alpha subunits (Figure 6f). The functional status of GlyR receptors on lOFC neurons was assessed by applying glycine locally to current-clamped neurons and monitoring changes

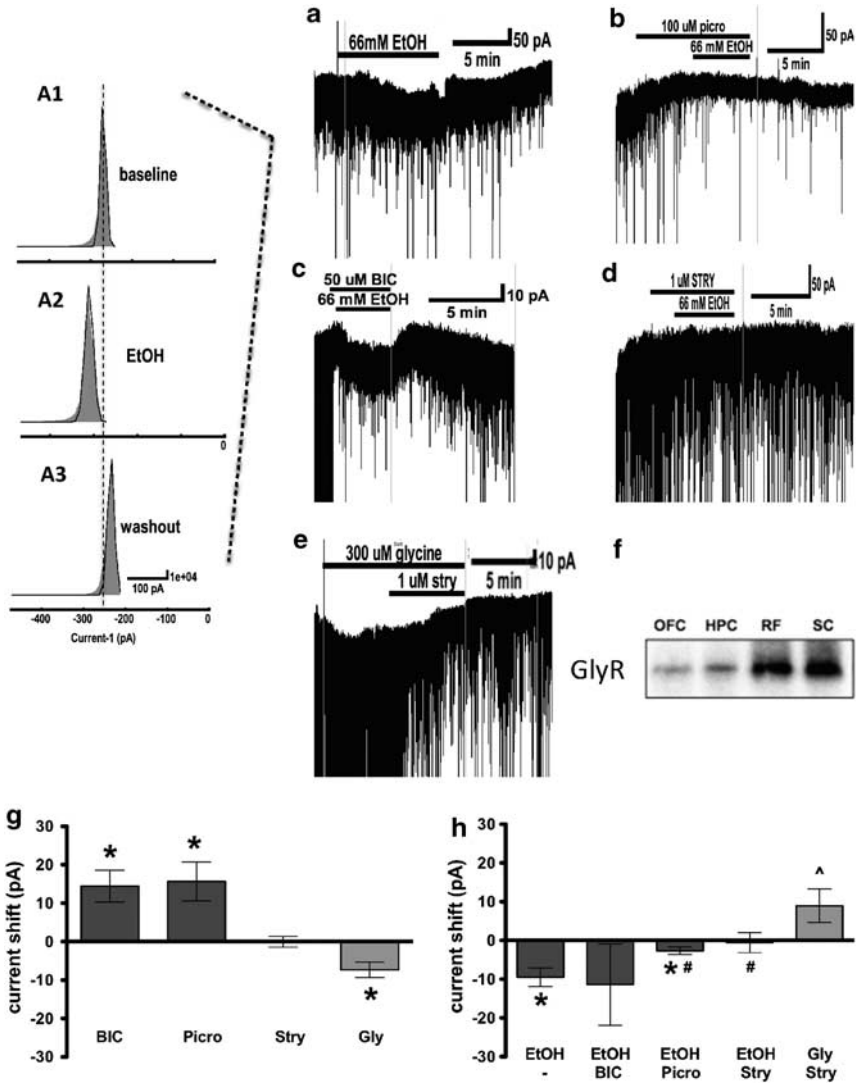

Figure 6 EtOH increases tonic current in lOFC neurons. Representative traces showing changes in holding current for (a) EtOH, (b) picrotoxin + EtOH, (c) bicuculline + EtOH, (d) strychnine + EtOH and (e) glycine + strychnine. In order to match the recording conditions used during the spiking studies (Figure 5), no pharmacological blocking agents were added to the recording aCSF in these experiments. Gaussian fit of tonic current amplitudes measured before, during and after EtOH exposure are shown in panels A1–A3. Vertical dashed lines in a1–a3 indicate baseline holding current values. (f) Representative western blot showing expression of glycine receptors in lOFC, hippocampus (HPC), reticular formation (RF) and spinal cord (SC). (g–h) Summary graphs show mean change in holding current (pA) each treatment group. Bars represent mean ± SEM. $N = 5$–8 for each treatment group. Symbols: * = differs from zero; # = differs from EtOH; ^ = differs from glycine.

in holding current. Glycine, at concentrations of 100 μM and below, had little effect on holding current (data not shown). However, at concentrations of 300 μM and higher, the holding current was significantly increased (Figures 6e and g). This glycine-induced change in holding current was reversed by the subsequent application of the glycine receptor antagonist strychnine (Figures 6e and h).

Effects of EtOH and Strychnine-sensitive Glycine Receptors on OFC Neuron Excitability

If a strychnine-sensitive glycine receptor current underlies EtOH's inhibition of OFC neuron excitability, then blocking these receptors should eliminate EtOH's effect on spike firing. To test this hypothesis, current-evoked spiking was measured in lOFC neurons in the presence and absence of EtOH and strychnine. As in the previous experiment, bath application of 33 mM EtOH significantly inhibited current-induced OFC neuron spike firing and this effect reversed upon washout (Treatment × Session: $F(2, 40) = 6.80$, $P < 0.05$; Figure 7). However, when recordings were performed in the presence of strychnine, EtOH had no significant effect on spike firing.

DISCUSSION

A major finding of this study is that a brief exposure to EtOH decreases current-evoked spike firing of lOFC neurons via a glycine receptor dependent mechanism. This effect occurred at EtOH concentrations that had no action on evoked or spontaneous GABA IPSCs and EtOH's effect

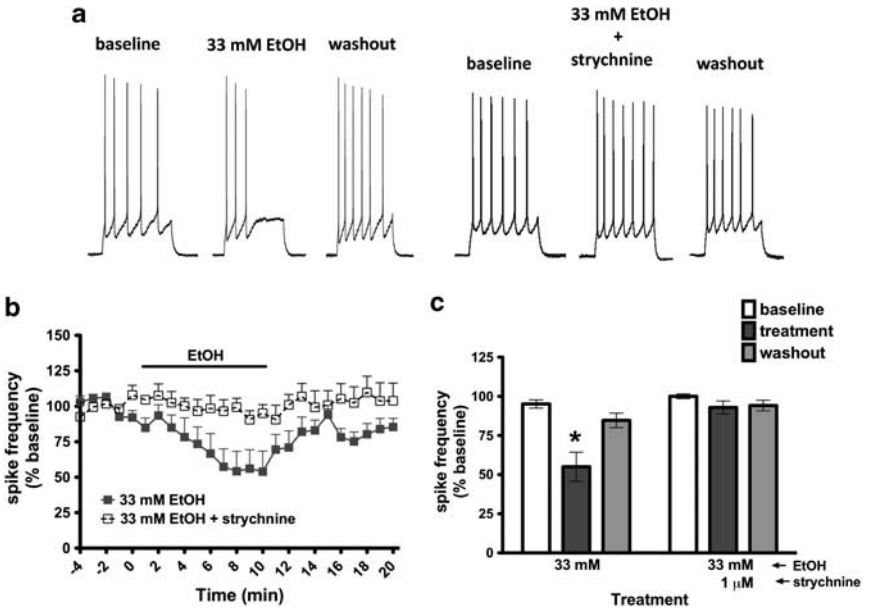

Figure 7 The glycine antagonist strychnine prevents EtOH-mediated inhibition of spiking in lOFC neurons. (a) Representative traces showing effects of EtOH (left panels) or EtOH plus the glycine antagonist strychnine (right panels) on current-induced spike firing. (b) Time-course of effects of 33 mM EtOH alone or 33 mM EtOH plus strychnine on spike frequency. Data are presented as percent of pre-drug baseline. (c) Summary chart showing effects of EtOH or EtOH plus strychnine on spike frequency during the last 2 min of each recording epoch (baseline, treatment, washout). Symbols: * = differs from all other groups. All bars and data points represent mean ± SEM. $N = 5–6$ for each treatment group.

on spike firing was not blocked by bicuculline, a selective $GABA_A$ receptor antagonist. At higher concentrations (66 mM), EtOH reduced NMDA but not AMPA-mediated EPSCs and this effect was maintained in the presence of a selective GluN2B antagonist. Together, these findings suggest that strychnine-sensitive glycine receptors and NMDA receptors may be important targets for the acute actions of EtOH on OFC function.

EtOH Decreases Intrinsic Excitability of OFC Neurons

Acute EtOH decreased the frequency of current-evoked action potentials in OFC neurons recorded from adult mice. This effect was accompanied by decreases in the input resistance of the recorded neurons and a modest hyperpolarization of the membrane potential. EtOH's effect on OFC neuron excitability was only slightly dose-dependent as all three concentrations tested (11, 33, 66 mM) had similar effects on spike frequency and input resistance. These values span the range of blood EtOH concentrations found in humans following light (0.05% BEC) to heavy (0.31% BEC) drinking and encompass those produced in alcohol-dependent mice ($\sim$0.18–0.225%; 40–50 mM) that, following withdrawal, express deficits in OFC-mediated cognitive flexibility (Badanich *et al*, 2011). Reports of EtOH affecting current-induced spike firing of neurons in other brain areas are mixed with some studies showing effects similar to the present study and others showing no effect. For example, in mouse thalamic slices, 50 mM EtOH reduced current-evoked neuronal firing but had no effect at 20 mM; a concentration just above the legal limit for intoxication in the US (Jia *et al*, 2008). Conversely, current-evoked spiking of deep layer neurons in brain slice cocultures of the medial PFC was unaffected by 100 mM EtOH (Tu *et al*, 2007). These brain regional differences in EtOH inhibition of spike firing are likely related to differences in the expression of EtOH-sensitive ion channels that influence neuronal excitability such as those activated by GABA and glycine.

In the present study, the inability of bicucculine to prevent EtOH inhibition of spike firing was somewhat surprising as a number of studies have implicated $GABA_A$ receptors as important targets of EtOH (reviewed by Weiner and Valenzuela, 2006). For example, in the (Jia *et al*, 2008) study mentioned above, EtOH's effect on spike firing was prevented by a selective $GABA_A$ antagonist that also blocked the EtOH-induced increase in tonic current. In thalamus, these tonic currents are likely mediated by $\alpha4\beta\delta$ receptors as they are potentiated by the δ-selective agonist THIP and are lost in mice devoid of $\alpha4$ $GABA_A$ subunits. The results from the present study suggest that while most lOFC neurons express biccuculine sensitive currents, these $GABA_A$ receptors are not sensitive to behaviorally relevant concentrations of EtOH. Thus, in lOFC neurons, the EtOH-induced increase in holding current was not blocked by biccuculine and spontaneous and evoked $GABA_A$ IPSCs were unaffected by EtOH up to concentrations of 66 mM. In a related study from this laboratory, EtOH also had no effect on GABA-mediated synaptic currents in layer V mPFC neurons and no evidence of an EtOH-sensitive tonic $GABA_A$ current was found in these neurons (Weitlauf and Woodward, 2008). Together, these findings highlight the diversity of EtOH's actions on GABA-mediated events and show that they are highly brain region and cell-type specific.

Unlike biccuculine, strychnine prevented EtOH's effect on lOFC neuron firing and the associated increase in holding current implying that glycine receptors mediate these effects. Immunohistochemical analysis showed that the lOFC expresses moderate amounts of GlyR protein although

the specific alpha subunits expressed could not be identified due to the lack of subunit-specific antibodies. In a recent study, PCR analysis revealed that GlyRα2 subunits dominate over α1 and α3 in frontal cortex, striatum and hippocampus in young animals and this profile is maintained in adulthood despite significant reductions in the overall expression of all subunits (Jonsson *et al*, 2012). A similar finding was reported for neurons in the basolateral amygdala (McCool and Farroni, 2001) suggesting that while α1 GlyRs are the dominant subtype in adult spinal cord (Lynch, 2009), α2 containing GlyRs may generate a significant population of functional neuronal GlyRs in higher brain areas. This conclusion is supported by findings from a recent study showing that dissociated rat PFC neurons generate robust glycine-activated currents that are strychnine-sensitive and exhibit an age-dependent change in picrotoxin sensitivity suggesting a loss of GlyRβ subunits (Lu and Ye, 2011). Together with the PCR data, these results suggest that neurons in frontal cortical areas may express substantial numbers of homomeric α2 GlyRs. This conclusion, although speculative, is important with respect to a possible mechanism of alcohol action on lOFC neurons as studies with recombinant subunits suggest that α1 GlyRs are considerably more sensitive to EtOH than α2 GlyRs. For example, at concentrations similar to those used in the present study ($\sim$5–50 mM), EtOH potentiated currents in oocytes expressing recombinant α1 GlyR receptors about twofold more than those expressing α2 GlyRs (Mascia *et al*, 1996) and similar findings have been reported for mammalian cells transfected with α1 or α2 GlyR subunits (Yevenes *et al*, 2010; but see Valenzuela *et al*, 1998). Although ethanol could augment ongoing glycine receptor function, we found no evidence for a tonic glycine receptor mediated current under control conditions as strychnine alone had no effect on the holding current of lOFC neurons. A similar finding was reported by (Zhang *et al*, 2008) who found no effect of strychnine on EPSP-spike (E-S) coupling in rat CA1 hippocampal pyramidal neurons; a measure that is sensitive to changes in neuronal excitability. In that study, spike coupling was reduced when 1 mM glycine was added to the bath and this effect was prevented by strychnine that by itself had no effect on the holding current. These findings support results from modeling studies showing that amino acid transporters can maintain extracellular levels of glycine at nanomolar levels (Attwell *et al*, 1993); well below the micromolar range of EC_{50} values reported for most GlyRs (Crawford *et al*, 2007; Mascia *et al*, 1996). Relevant to this finding is a report showing that n-alkanols, including EtOH selectively inhibit glycine transporters expressed in HEK cells (Nunez *et al*, 2000). Such an effect, by increasing extracellular levels of glycine, might also account for EtOH's ability to inhibit spike firing of lOFC neurons. However, this seems unlikely for several reasons. First, the concentration of EtOH reported to inhibit glycine transporter function was 100 mM or greater, well above that found in the present study to reduce spiking. Secondly, this effect was restricted to the neuronal GlyT2 subtype that is present in presynaptic glycine neuron terminals that are absent in most cortical areas (Zeilhofer *et al*, 2005). Finally, although most brain areas also express the glial GlyT1 form of the transporter, glycine uptake by these carriers was unaffected by EtOH up to 400 mM (Nunez *et al*, 2000). These findings suggest that other mechanisms may be involved in mediating EtOH's actions on lOFC excitability.

In addition to glycine, GlyRs are also activated by other endogenous amino acids including taurine and beta-alanine. In particular, taurine is present in high concentrations in brain and acts as a partial agonist at GlyR receptors (Wu and Prentice, 2010). Microdialysis studies reveal that EtOH applied systemically or locally induces a rapid increase in extracellular taurine levels in the nucleus accumbens (Adermark *et al*, 2011; Smith *et al*, 2004) with much less effect in dorsal striatum (Smith *et al*, 2004) suggesting brain regional differences in EtOH-taurine interactions. The mechanisms underlying this effect are not completely known but may involve an EtOH-induced increase in astrocyte volume that triggers a release of taurine in order to maintain osmotic pressure in these cells. For example, (Adermark *et al*, 2011) showed that EtOH caused swelling in 15–17% of cultured rat astrocytes and that this effect was similar for both 25 and 50 mM EtOH. These concentrations are within the range of those found in the present study (11–66 mM) to reduce spike firing of lOFC neurons. Thus, while speculative at this point, glial-derived taurine may be one factor that underlies the EtOH-induced modulation of spike firing of lOFC neurons.

EtOH Inhibits Synaptic NMDA Receptor Function

In addition to its effects on current-induced spike firing, EtOH also inhibited synaptic NMDA currents in lOFC neurons. This finding is consistent with other reports showing that EtOH decreases the amplitude of NMDA EPSCs in various brain regions including the mPFC (Weitlauf and Woodward, 2008), hippocampus (Lovinger *et al*, 1990), amygdala (Roberto *et al*, 2004), BNST (Kash *et al*, 2008), and striatum (Wang *et al*, 2007). In the present study, 66 mM EtOH significantly inhibited NMDA EPSCs while lower EtOH concentrations (11, 33 mM) had little effect suggesting that NMDA receptors in the adult OFC, unlike some areas, are not particularly sensitive to EtOH. For example, NMDA mediated EPSCs in the medial PFC and BNST were significantly inhibited by 22–25 mM EtOH (Kash *et al*, 2008; Weitlauf and Woodward, 2008). It is unlikely that these findings can be fully accounted for by age or species differences between these studies as adult mice were used as the source of lOFC and BNST neurons while adolescent rats were used in the mPFC study. Studies using recombinant expression systems have suggested that subunit composition, especially GluN2B, can influence the degree of EtOH inhibition of NMDA receptors. However, these data are mixed with some reports showing enhanced sensitivity of GluN2B receptors (Anders *et al*, 1999; Blevins *et al*, 1997; Lovinger, 1995), others reporting no difference (Chu *et al*, 1995; Kuner *et al*, 1993; Otton *et al*, 2009) and one showing that GluN1 splice variants also influences overall sensitivity (Jin and Woodward, 2006). Support for a role of EtOH-sensitive GluN2B subunits in neurons comes from brain slice studies showing that EtOH has little effect on NMDA EPSCs recorded in the presence of selective GluN2B antagonists (Kash *et al*, 2008; Roberto *et al*, 2004) or from GluN2B conditional knockout mice (Wills *et al*, 2012). However, unlike NMDA currents in those reports

that were recorded from central amygdala and BNST, NMDA EPSCs in lOFC neurons and hippocampus (Suvarna *et al*, 2005) are significantly inhibited by EtOH even in the presence of Ro-25-6981 that by itself reduces the amplitude of NMDA evoked responses. These findings point out that while subunit composition may influence the overall EtOH sensitivity of NMDA receptors in some brain regions, other factors such as those related to receptor phosphorylation and trafficking (Alvestad *et al*, 2003; Wu *et al*, 2011; Yaka *et al*, 2003) may contribute to EtOH's action on neuronal NMDA receptors.

Summary

Overall, the results of this study show that EtOH concentrations associated with mild to moderate drinking have only modest effects on glutamatergic transmission of lOFC neurons but markedly inhibit current-evoked spiking. This action is blocked by strychnine, a glycine receptor antagonist that by itself has no effect on spike activity or tonic current. Combined with the minimal effects of EtOH on GABAergic mediated phasic and tonic signaling, these results show that lOFC neurons have a profile of EtOH sensitivity that is distinct from that reported in other brain regions and predict that repeated exposures to EtOH may induce novel changes in markers of neuronal excitability in lOFC neurons.

ACKNOWLEDGEMENTS

This work was supported by grants to KAB (F32 AA019610) and JJW (P50 AA010761; RC3; R37 AA009986).

DISCLOSURE

The authors declare no conflict of interest.

REFERENCES

Adermark L, Clarke RB, Olsson T, Hansson E, Soderpalm B, Ericson M (2011). Implications for glycine receptors and astrocytes in ethanol-induced elevation of dopamine levels in the nucleus accumbens. *Addict Biol* **16**: 43–54.

Adinoff B (2004). Neurobiologic processes in drug reward and addiction. *Harv Rev Psychiatry* **12**: 305–320.

Alvestad RM, Grosshans DR, Coultrap SJ, Nakazawa T, Yamamoto T, Browning MD (2003). Tyrosine dephosphorylation and ethanol inhibition of N-Methyl-D-aspartate receptor function. *J Biol Chem* **278**: 11020–11025.

Anders DL, Blevins T, Sutton G, Chandler LJ, Woodward JJ (1999). Effects of c-Src tyrosine kinase on ethanol sensitivity of recombinant NMDA receptors expressed in HEK 293 cells. *Alcohol Clin Exp Res* **23**: 357–362.

Attwell D, Barbour B, Szatkowski M (1993). Nonvesicular release of neurotransmitter. *Neuron* **11**: 401–407.

Badanich KA, Becker HC, Woodward JJ (2011). Effects of chronic intermittent ethanol exposure on orbitofrontal and medial prefrontal cortex-dependent behaviors in mice. *Behav Neurosci* **125**: 879–891.

Bechara A, Damasio H, Tranel D, Anderson SW (1998). Dissociation Of working memory from decision making within the human prefrontal cortex. *J Neurosci* **18**: 428–437.

Bissonette GB, Martins GJ, Franz TM, Harper ES, Schoenbaum G, Powell EM (2008). Double dissociation of the effects of medial and orbital prefrontal cortical lesions on attentional and affective shifts in mice. *J Neurosci* **28**: 11124–11130.

Blevins T, Mirshahi T, Chandler LJ, Woodward JJ (1997). Effects of acute and chronic ethanol exposure on heteromeric N-methyl-D-aspartate receptors expressed in HEK 293 cells. *J Neurochem* **69**: 2345–2354.

Boettiger CA, Mitchell JM, Tavares VC, Robertson M, Joslyn G, D'Esposito M *et al* (2007). Immediate reward bias in humans: fronto-parietal networks and a role for the catechol-O-methyltransferase 158(Val/Val) genotype. *J Neurosci* **27**: 14383–14391.

Bokura H, Yamaguchi S, Kobayashi S (2001). Electrophysiological correlates for response inhibition in a Go/NoGo task. *Clin Neurophysiol* **112**: 2224–2232.

Chu B, Anantharam V, Treistman SN (1995). Ethanol inhibition of recombinant heteromeric NMDA channels in the presence and absence of modulators. *J Neurochem* **65**: 140–148.

Crawford DK, Trudell JR, Bertaccini EJ, Li K, Davies DL, Alkana RL (2007). Evidence that ethanol acts on a target in Loop 2 of the extracellular domain of alpha1 glycine receptors. *J Neurochem* **102**: 2097–2109.

Cummings JL (1995). Anatomic and behavioral aspects of frontal-subcortical circuits. *Ann N Y Acad Sci* **769**: 1–13.

Dalley JW, Cardinal RN, Robbins TW (2004). Prefrontal executive and cognitive functions in rodents: neural and neurochemical substrates. *Neurosci Biobehav Rev* **28**: 771–784.

Dias-Ferreira E, Sousa JC, Melo I, Morgado P, Mesquita AR, Cerqueira JJ *et al* (2009). Chronic stress causes frontostriatal reorganization and affects decision-making. *Science* **325**: 621–625.

Franklin KBJ, Paxinos G (2008). *The mouse brain in stereotaxic coordinates*. 3rd edn. Boston: Elsevier/Academic Press: Amsterdam, 1 v. (various pagings)pp.

Glykys J, Peng Z, Chandra D, Homanics GE, Houser CR, Mody I (2007). A new naturally occurring GABA(A) receptor subunit partnership with high sensitivity to ethanol. *Nat Neurosci* **10**: 40–48.

Hill SY, Wang S, Kostelnik B, Carter H, Holmes B, McDermott M *et al* (2009). Disruption of orbitofrontal cortex laterality in offspring from multiplex alcohol dependence families. *Biol Psychiatry* **65**: 129–136.

Ikeda A, Luders HO, Collura TF, Burgess RC, Morris HH, Hamano T *et al* (1996). Subdural potentials at orbitofrontal and mesial prefrontal areas accompanying anticipation and decision making in humans: a comparison with Bereitschaftspotential. *Electroencephalogr Clin Neurophysiol* **98**: 206–212.

Ito S, Ohgushi M, Ifuku H, Ogawa H (2001). Neuronal activity in the monkey fronto-opercular and adjacent insular/prefrontal cortices during a taste discrimination GO/NOGO task: response to cues. *Neurosci Res* **41**: 257–266.

Jia F, Chandra D, Homanics GE, Harrison NL (2008). Ethanol modulates synaptic and extrasynaptic GABAA receptors in the thalamus. *J Pharmacol Exp Ther* **326**: 475–482.

Jin C, Woodward JJ (2006). Effects of 8 different NR1 splice variants on the ethanol inhibition of recombinant NMDA receptors. *Alcohol Clin Exp Res* **30**: 673–679.

Jonsson S, Morud J, Pickering C, Adermark L, Ericson M, Soderpalm B (2012). Changes in glycine receptor subunit expression in forebrain regions of the Wistar rat over development. *Brain Res* **1446**: 12–21.

Kash TL, Matthews RT, Winder DG (2008). Alcohol inhibits NR2B-containing NMDA receptors in the ventral bed nucleus of the stria terminalis. *Neuropsychopharmacology* **33**: 1379–1390.

Kuner T, Schoepfer R, Korpi ER (1993). Ethanol inhibits glutamate-induced currents in heteromeric NMDA receptor subtypes. *Neuroreport* **5**: 297–300.

Liston C, Miller MM, Goldwater DS, Radley JJ, Rocher AB, Hof PR *et al* (2006). Stress-induced alterations in prefrontal cortical

dendritic morphology predict selective impairments in perceptual attentional set-shifting. *J Neurosci* **26**: 7870–7874.

Lovinger DM (1995). Developmental decrease in ethanol inhibition of N-methyl-D-aspartate receptors in rat neocortical neurons: relation to the actions of ifenprodil. *J Pharmacol Exp Ther* **274**: 164–172.

Lovinger DM, White G, Weight FF (1990). NMDA receptor-mediated synaptic excitation selectively inhibited by ethanol in hippocampal slice from adult rat. *J Neurosci* **10**: 1372–1379.

Lu Y, Ye JH (2011). Glycine-activated chloride currents of neurons freshly isolated from the prefrontal cortex of young rats. *Brain Res* **1393**: 17–22.

Lynch JW (2009). Native glycine receptor subtypes and their physiological roles. *Neuropharmacology* **56**: 303–309.

Mascia MP, Mihic SJ, Valenzuela CF, Schofield PR, Harris RA (1996). A single amino acid determines differences in ethanol actions on strychnine-sensitive glycine receptors. *Mol Pharmacol* **50**: 402–406.

McCool BA, Farroni JS (2001). Subunit composition of strychnine-sensitive glycine receptors expressed by adult rat basolateral amygdala neurons. *Eur J Neurosci* **14**: 1082–1090.

McGaughy J, Ross RS, Eichenbaum H (2008). Noradrenergic, but not cholinergic, deafferentation of prefrontal cortex impairs attentional set-shifting. *Neuroscience* **153**: 63–71.

Nunez E, Lopez-Corcuera B, Martinez-Maza R, Aragon C (2000). Differential effects of ethanol on glycine uptake mediated by the recombinant GLYT1 and GLYT2 glycine transporters. *Br J Pharmacol* **129**: 802–810.

Otton HJ, Janssen A, O'Leary T, Chen PE, Wyllie DJ (2009). Inhibition of rat recombinant GluN1/GluN2A and GluN1/GluN2B NMDA receptors by ethanol at concentrations based on the US/UK drink-drive limit. *Eur J Pharmacol* **614**: 14–21.

Ramus SJ, Eichenbaum H (2000). Neural correlates of olfactory recognition memory in the rat orbitofrontal cortex. *J Neurosci* **20**: 8199–8208.

Roberto M, Madamba SG, Moore SD, Tallent MK, Siggins GR (2003). Ethanol increases GABAergic transmission at both pre- and postsynaptic sites in rat central amygdala neurons. *Proc Natl Acad Sci USA* **100**: 2053–2058.

Roberto M, Schweitzer P, Madamba SG, Stouffer DG, Parsons LH, Siggins GR (2004). Acute and chronic ethanol alter glutamatergic transmission in rat central amygdala: an *in vitro* and *in vivo* analysis. *J Neurosci* **24**: 1594–1603.

Roesch MR, Calu DJ, Burke KA, Schoenbaum G (2007a). Should I stay or should I go? Transformation of time-discounted rewards in orbitofrontal cortex and associated brain circuits. *Ann N Y Acad Sci* **1104**: 21–34.

Roesch MR, Stalnaker TA, Schoenbaum G (2007b). Associative encoding in anterior piriform cortex versus orbitofrontal cortex during odor discrimination and reversal learning. *Cereb Cortex* **17**: 643–652.

Schoenbaum G, Chiba AA, Gallagher M (1998). Orbitofrontal cortex and basolateral amygdala encode expected outcomes during learning. *Nat Neurosci* **1**: 155–159.

Schoenbaum G, Eichenbaum H (1995). Information coding in the rodent prefrontal cortex. I. Single-neuron activity in orbitofrontal cortex compared with that in pyriform cortex. *J Neurophysiol* **74**: 733–750.

Schultz W, Tremblay L, Hollerman JR (2000). Reward processing in primate orbitofrontal cortex and basal ganglia. *Cereb Cortex* **10**: 272–284.

Smith A, Watson CJ, Frantz KJ, Eppler B, Kennedy RT, Peris J (2004). Differential increase in taurine levels by low-dose ethanol in the dorsal and ventral striatum revealed by microdialysis with on-line capillary electrophoresis. *Alcohol Clin Exp Res* **28**: 1028–1038.

Suvarna N, Borgland SL, Wang J, Phamluong K, Auberson YP, Bonci A *et al* (2005). Ethanol alters trafficking and functional N-methyl-D-aspartate receptor NR2 subunit ratio via H-Ras. *J Biol Chem* **280**: 31450–31459.

Tanabe J, Tregellas JR, Dalwani M, Thompson L, Owens E, Crowley T *et al* (2009). Medial orbitofrontal cortex gray matter is reduced in abstinent substance-dependent individuals. *Biol Psychiatry* **65**: 160–164.

Thorpe SJ, Rolls ET, Maddison S (1983). The orbitofrontal cortex: neuronal activity in the behaving monkey. *Exp Brain Res* **49**: 93–115.

Tremblay L, Schultz W (1999). Relative reward preference in primate orbitofrontal cortex. *Nature* **398**: 704–708.

Tu Y, Kroener S, Abernathy K, Lapish C, Seamans J, Chandler LJ *et al* (2007). Ethanol inhibits persistent activity in prefrontal cortical neurons. *J Neurosci* **27**: 4765–4775.

Valenzuela CF, Cardoso RA, Wick MJ, Weiner JL, Dunwiddie TV, Harris RA (1998). Effects of ethanol on recombinant glycine receptors expressed in mammalian cell lines. *Alcohol Clin Exp Res* **22**: 1132–1136.

Verdejo-Garcia A, Bechara A, Recknor EC, Perez-Garcia M (2006). Executive dysfunction in substance dependent individuals during drug use and abstinence: an examination of the behavioral, cognitive and emotional correlates of addiction. *J Int Neuropsychol Soc* **12**: 405–415.

Wang DS, Mangin JM, Moonen G, Rigo JM, Legendre P (2006). Mechanisms for picrotoxin block of alpha2 homomeric glycine receptors. *J Biol Chem* **281**: 3841–3855.

Wang J, Carnicella S, Phamluong K, Jeanblanc J, Ronesi JA, Chaudhri N *et al* (2007). Ethanol induces long-term facilitation of NR2B-NMDA receptor activity in the dorsal striatum: implications for alcohol drinking behavior. *J Neurosci* **27**: 3593–3602.

Wei W, Faria LC, Mody I (2004). Low ethanol concentrations selectively augment the tonic inhibition mediated by delta subunit-containing GABAA receptors in hippocampal neurons. *J Neurosci* **24**: 8379–8382.

Weiner JL, Valenzuela CF (2006). Ethanol modulation of GABAergic transmission: the view from the slice. *Pharmacol Ther* **111**: 533–554.

Weitlauf C, Woodward JJ (2008). Ethanol selectively attenuates NMDAR-mediated synaptic transmission in the prefrontal cortex. *Alcohol Clin Exp Res* **32**: 690–698.

Wills TA, Klug JR, Silberman Y, Baucum AJ, Weitlauf C, Colbran RJ *et al* (2012). GluN2B subunit deletion reveals key role in acute and chronic ethanol sensitivity of glutamate synapses in bed nucleus of the stria terminalis. *Proc Natl Acad Sci USA* **109**: E278–E287.

Wu JY, Prentice H (2010). Role of taurine in the central nervous system. *J Biomed Sci* **17**(Suppl 1): S1.

Wu PH, Coultrap SJ, Browning MD, Proctor WR (2011). Functional adaptation of the N-methyl-D-aspartate receptor to inhibition by ethanol is modulated by striatal-enriched protein tyrosine phosphatase and p38 mitogen-activated protein kinase. *Mol Pharmacol* **80**: 529–537.

Yaka R, Phamluong K, Ron D (2003). Scaffolding of Fyn kinase to the NMDA receptor determines brain region sensitivity to ethanol. *J Neurosci* **23**: 3623–3632.

Yevenes GE, Moraga-Cid G, Avila A, Guzman L, Figueroa M, Peoples RW *et al* (2010). Molecular requirements for ethanol differential allosteric modulation of glycine receptors based on selective Gbetagamma modulation. *J Biol Chem* **285**: 30203–30213.

Zeilhofer HU, Studler B, Arabadzisz D, Schweizer C, Ahmadi S, Layh B *et al* (2005). Glycinergic neurons expressing enhanced green fluorescent protein in bacterial artificial chromosome transgenic mice. *J Comp Neurol* **482**: 123–141.

Zhang LH, Gong N, Fei D, Xu L, Xu TL (2008). Glycine uptake regulates hippocampal network activity via glycine receptor-mediated tonic inhibition. *Neuropsychopharmacology* **33**: 701–711.